Chapter 16
Temporal Variation

Abstract IDE models naturally allow a certain temporal variation within a generation since they divide each generation into separate growth and dispersal phases. However, so far we have assumed that the growth phases in all generations are identical and that the same holds for the dispersal phases. In realistic environments, external conditions in subsequent generations may vary substantially so that growth and dispersal behavior could differ. In this chapter, we present some theory on and examples of how to formulate and analyze IDEs with a periodically or randomly varying growth function and dispersal kernel. In the periodic case, much of the previous theory for temporally constant environments can be applied to the period map. In the random case, even the formulation of the problem requires substantially different tools from the theory of stochastic processes. We focus again on the two fundamental questions of population persistence and spread.

16.1 Nonspatial Models with Temporal Variation

We illustrate and explain some basic questions about how temporal variation affects population dynamics by using the simple nonspatial model from (2.3). We also introduce some terminology for subsequent spatial models. We denote the population density in year t by N_t and the temporally varying growth function by F_t. We study the dynamics of the equation

$$N_{t+1} = F_t(N_t) \tag{16.1}$$

when the environment varies periodically or randomly in time.

Periodic Variation

When the environment is periodic with period $T \in \mathbb{N}$, we can study the map of the Tth iteration

© Springer Nature Switzerland AG 2019

F. Lutscher, *Integrodifference Equations in Spatial Ecology*, Interdisciplinary Applied Mathematics 49, https://doi.org/10.1007/978-3-030-29294-2_16

$$N_{t+T} = G(N_t) = F_{t+T-1} \circ F_{t+T-2} \circ \cdots \circ F_{t+1} \circ F_t(N_t) \tag{16.2}$$

with the usual techniques for discrete maps. The qualitative behavior of this map is independent of the choice of t.

For an example, we consider a two-periodic environment with growth functions

$$F_i(N) = \frac{R_i N}{1 + \kappa_i N}, \qquad i = 1, 2, \tag{16.3}$$

from (2.11) with $R_i, \kappa_i > 0$. Since F_i are monotone increasing and concave down, $G = F_2 \circ F_1$ has the same properties. Therefore, the dynamics of (16.2) are determined by the local stability of the zero state. If the zero state is locally stable, then it is globally stable; if it is unstable, then there is a globally stable positive steady state; see Sect. 2.2. The linearization of G at $N = 0$ is given by

$$n_{t+2} = R_2 R_1 n_t, \tag{16.4}$$

so that the zero state is unstable if and only if $R_2 R_1 > 1$. If this condition is satisfied, the positive steady state of G is given by

$$N^* = \frac{R_2 R_1 - 1}{\kappa_1 + \kappa_2 R_1}. \tag{16.5}$$

The solutions of the original system, $N_{t+1} = F_t(N_t)$, will converge to zero if $R_2 R_1 < 1$ and will approach a positive stable two-cycle, (N_1^*, N_2^*), when the inequality is reversed. One of the two states of the two-cycle is given by N^* above and the other by the corresponding expression with all indices exchanged.

Stochastic Variation

When the environment varies randomly, the formulation of the equations and the terminology and techniques used to study them are based on stochastic processes and differ considerably from the deterministic theory covered in previous chapters. We refer to Allen (2010) or Meyn and Tweedie (2009) for a thorough introduction.

We begin with the linear model

$$N_{t+1} = R_t N_t, \qquad t = 0, 1, 2, \ldots, \tag{16.6}$$

and follow the exposition by Lewis et al. (2016). We assume that R_t are finite positive random variables that are independent and identically distributed (iid) with finite positive expectation $E[R_t] = E[R_0]$ for all t. As usual, R_t is the per capita growth rate of the population, i.e., the average number of offspring that an individual has in the given year, t. Since R_t are random variables, so are N_t, and we can ask

for their expectation, denoted by $E[N_t]$. Under the assumption that environmental conditions are independent of population density, we have

$$E[N_{t+1}] = E[R_t N_t] = E[R_t]E[N_t]\,. \tag{16.7}$$

Hence, the expected population density satisfies a deterministic equation with growth rate $E[R_0]$. Its solution is explicitly given by

$$E[N_t] = E[N_0]E[R_0]^t = E[N_0]\mathrm{e}^{t\ln E[R_0]}\,. \tag{16.8}$$

It will grow in time when the geometric growth rate satisfies $E[R_0] > 1$ or the arithmetic growth rate $\ln(E[R_0]) > 0$.

On the other hand, we can write the solution of (16.6) explicitly as

$$N_t = N_0 \prod_{j=0}^{t-1} R_j = N_0 \exp\left(t\,\frac{1}{t}\sum_{j=0}^{t-1} \ln R_j \right). \tag{16.9}$$

Hence, the expected arithmetic growth rate is $E[\ln(R_0)]$. The process will grow to infinity with probability one if $E[\ln(R_0)] > 0$ and decay to zero with probability one if the reverse inequality holds. Since the logarithm is a concave function, Jensen's inequality states that $E[\ln(R_0)] \le \ln(E[R_0])$. Hence, it is possible that the expectation in (16.8) is predicted to grow, whereas the actual solution in (16.9) will decay to zero with probability one.

We present an example similar to the two-periodic example above. We assume that the growth rate is a Bernoulli random variable that assumes values R_1 and R_2 with probability p and $1-p$, respectively. Clearly, the population can grow when $R_{1,2} > 1$. However, if we choose $R_1 > 1 > R_2 > 0$, we find two threshold probabilities. We have

$$\ln(E[R_0]) > 0 \quad \text{if and only if} \quad p > p^* = \frac{1-R_2}{R_1-R_2} \tag{16.10}$$

and

$$E[\ln(R_0)] > 0 \quad \text{if and only if} \quad p > p^{**} = \frac{-\ln(R_2)}{\ln(R_1)-\ln(R_2)}\,. \tag{16.11}$$

For example, choosing $R_1 = 2$ and $R_2 = 1/4$ gives $p^* = 3/7 < 1/2 < 2/3 = p^{**}$. For $p \in (p^*, p^{**})$, the expectation in (16.8) will grow but the solution in (16.9) will decay to zero with probability one.

The study of nonlinear stochastic processes is more complicated. It requires concepts and results that we cannot introduce in detail here; see, e.g., Allen (2010) or Meyn and Tweedie (2009). Instead, we briefly discuss the results on the

stochastic version of the Beverton–Holt equation from Ellner (1984). We present their generalization to IDEs in Sect. 16.3.

Ellner (1984) considers model (16.1) with $F_t(N) = F(N, \alpha_t)$, where α_t represents parameters in F that describe the random environment in year t. He assumes that α_t are iid random variables. Then N_t is a homogeneous Markov process. It turns out that if F has properties like the Beverton–Holt function, then stability results similar to the deterministic case hold for the stochastic case. Of course, instead of a stationary state, we now have a stationary distribution. More precisely, we assume that F is differentiable, monotone increasing, concave, and bounded for each possible random environment. Then the stochastic process N_t has a stationary distribution, μ_*, independent of N_0. There are two possibilities. The first is $\mu_*(\{0\}) = 1$, which means that the entire mass of the stationary distribution is concentrated at $N = 0$. In this case, the process will die out with probability one. The second possibility is $\mu_*(\{0\}) = 0$, which means that the stationary distribution is supported in $(0, \infty)$. In this case, the process will persist with probability one. The behavior of the process is decided by the linear process $n_{t+1} = F'(0, \alpha_t)n_t$. If $E[\ln(F'(0, \alpha_t)] < 0$, the process will die out with probability one. If the inequality is reversed, the process will persist. The results in Ellner (1984) are formulated for more general growth functions.

16.2 The Gaussian Habitat Quality Model with Temporal Variation

We begin our study of the effects of temporal variation on population persistence in a spatial model with an explicitly solvable model, namely the linear model in (15.4) with Gaussian habitat quality function (Latore et al. 1999). Even with temporally varying parameters, this model can be reduced to a two-dimensional difference equation as in Proposition 15.1. The ideas and concepts from the preceding section can then be applied to study the spatial problem as well.

Our model equation is

$$N_{t+1}(x) = R_t \mathrm{e}^{-x^2/(2\rho_t^2)} \int_{-\infty}^{\infty} K_G(x - y; \sigma_t^2) N_t(y) \mathrm{d}y \,, \tag{16.12}$$

where K_G is the Gaussian dispersal kernel. Parameters R_t, ρ_t^2, and σ_t^2 depend on time. As before, R_t is the per capita reproduction rate in year t, ρ_t^2 measures the extent of the habitat in year t, and σ_t^2 is the variance of the dispersal kernel in year t. All parameters are assumed positive.

As in Proposition 15.1, model (16.12) has a solution of the form $N_t = A_t \exp(-\frac{x^2}{2\nu_t^2})$, where A_t and ν_t^2 satisfy the difference equations

$$\nu_{t+1}^2 = F_t(\nu_t^2) := \frac{\rho_t^2(\sigma_t^2 + \nu_t^2)}{\rho_t^2 + \sigma_t^2 + \nu_t^2} \quad \text{and} \quad A_{t+1} = A_t R_t \sqrt{\frac{\nu_t^2}{\sigma_t^2 + \nu_t^2}}\,. \tag{16.13}$$

Function F_t is differentiable, monotone increasing, concave down, bounded, and positive for $\nu_t^2 > 0$.

Periodic Variation

When the environment is periodic, we can obtain explicit conditions for population persistence and thereby study trade-offs between "good" and "bad" years. We consider a two-periodic environment and denote the respective values of the parameters by $R_{1,2}$, $\rho_{1,2}^2$, and $\sigma_{1,2}^2$, as well as functions $F_{1,2}$. By the considerations in the preceding section, the iteration for ν_t^2 converges to a stable two-cycle, (ν_{1*}^2, ν_{2*}^2). Here, ν_{1*}^2 is the positive solution of the quadratic

$$\begin{aligned}\left(\rho_1^2 + \rho_2^2 + \sigma_2^2\right)\nu_{1*}^4 + \left(\rho_1^2\sigma_1^2 - \rho_2^2\sigma_2^2 + \rho_1^2\sigma_2^2 + \rho_2^2\sigma_1^2 + \sigma_1^2\sigma_2^2\right)\nu_{1*}^2 \\ - \left(\rho_1^2\rho_2^2\sigma_1^2 + \rho_1^2\rho_2^2\sigma_2^2 + \rho_1^2\sigma_1^2\sigma_2^2\right) = 0\end{aligned} \tag{16.14}$$

and $\nu_{2*}^2 = F_1(\nu_{1*}^2)$. Hence, the iteration for A_t approaches the linear function

$$A_{t+1} = A_t R_j \sqrt{\frac{\nu_{j*}^2}{\nu_{j*}^2 + \sigma_j^2}}\,, \tag{16.15}$$

with $j = 1$ if t is odd and $j = 2$ if t is even.

According to the results from the preceding section, A_t will grow eventually if and only if

$$R_1 R_2 > \sqrt{\left(1 + \frac{\sigma_1^2}{\nu_{1*}^2}\right)\left(1 + \frac{\sigma_2^2}{\nu_{2*}^2}\right)}\,. \tag{16.16}$$

For a temporally constant habitat with $R_1 = R_2$, $\sigma_1 = \sigma_2$, and $\rho_1 = \rho_2$, this condition is just the persistence condition from (15.12).

We explore the persistence condition as follows. We express $\sigma_{1,2}^2 = \bar{\sigma}^2 \pm \epsilon_\sigma$ in terms of the mean, $\bar{\sigma}^2$, and deviation, ϵ_σ, and similarly for $\rho_{1,2}^2 = \bar{\rho}^2 \pm \epsilon_\rho$. Figure 16.1 shows the contour lines of the critical value of $R_1 R_2$ that guarantees persistence according to (16.16). We observe that variation in suitable habitat size alone ($\epsilon_\rho > 0$, $\epsilon_\sigma = 0$) requires a higher growth rate for persistence, whereas variation in dispersal distance only ($\epsilon_\rho = 0$, $\epsilon_\sigma > 0$) allows for a lower growth rate.

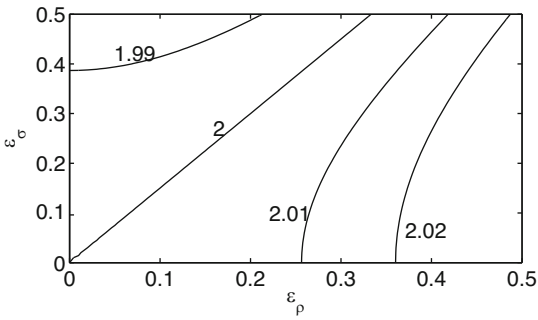

Fig. 16.1 Contour lines for persistence condition (16.16) with $\sigma^2_{1,2} = 1 \pm \epsilon_\sigma$ and $\rho^2_{1,2} = 2 \pm \epsilon_\rho$. The numbers on the contour lines indicate the threshold values. The persistence threshold in the absence of temporal variation is $R_1 R_2 = 2$.

When both parameters vary simultaneously, the joint effect depends on the relative strength (variation) of the two.

Stochastic Variation

Now we assume that environmental conditions vary randomly, and we describe the corresponding growth rate, habitat size, and dispersal behavior by positive random variables R_t, ρ_t^2, and σ_t^2, each of which is assumed iid with positive finite expectation. According to Theorem 2.2 by Ellner (1984), ν_t^2 converges to a stationary distribution, supported on $(0, \infty)$.

The equation for A_t can be solved explicitly as

$$A_t = A_0 \prod_{j=0}^{t-1} R_j \sqrt{\frac{\nu_j^2}{\nu_j^2 + \sigma_j^2}}\,, \tag{16.17}$$

which gives

$$\ln\left(\frac{A_t}{A_0}\right) = t\left(E[\ln(R_t)] + \frac{1}{2}E\left[\ln\left(\frac{\nu_t^2}{\nu_t^2 + \sigma_t^2}\right)\right]\right). \tag{16.18}$$

The population eventually grows with probability one if the term on the right-hand side is positive in the limit as $t \to \infty$. We can write this condition suggestively as

$$E[\ln(R_0)] > \frac{1}{2}E\left[\ln\left(1 + \frac{\sigma_0^2}{\nu_*^2}\right)\right], \tag{16.19}$$

where ν_*^2 stands for a random variable whose distribution equals the stationary distribution of the variables ν_t^2.

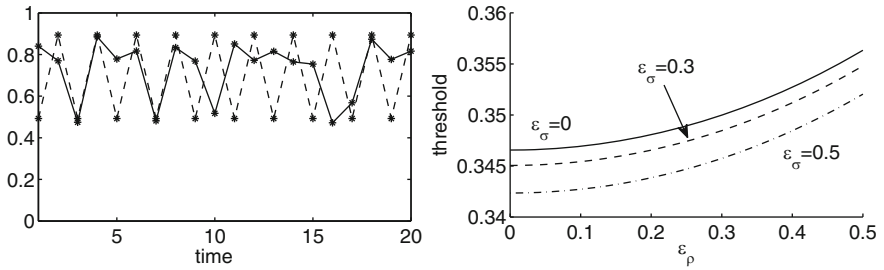

Fig. 16.2 **Left:** The expression $\ln(1 + \sigma_t^2/\nu_t^2)$ from (16.18) in the periodic case (dashed) and one realization of the corresponding stochastic case (solid). **Right:** Persistence threshold (16.19) as a function of ϵ_ρ for $\epsilon_\sigma = 0$ (solid), $\epsilon_\sigma = 0.3$ (dashed), and $\epsilon_\sigma = 0.5$ (dash-dot). The plot was obtained by simulating the stochastic process for up to 10,000 time steps and calculating the expectation numerically.

We can evaluate this condition numerically. We use the setup that most closely resembles the periodic model: ρ_t^2, σ_t^2 are Bernoulli random variables, where the two possible values $\rho_{1,2}^2$ and $\sigma_{1,2}^2$ appear with equal probability. We keep the mean of each variable fixed and vary the deviation. It turns out that the resulting persistence condition in (16.19) is exactly the same as the one in (16.16). In Fig. 16.2, we plot one realization of the process and compare it to the periodic case (left panel). We also plot the threshold condition from (16.19) as a function of ϵ_ρ, the deviation of ρ^2. Each curve increases with ϵ_ρ, indicating that persistence is harder to achieve as the variation in ρ^2 increases. However, for fixed ϵ_ρ, the threshold decreases with ϵ_σ, indicating that persistence is easier to achieve as the variation in σ^2 increases. The thresholds from the stochastic process and the periodic case are indistinguishable.

16.3 Persistence Under Temporal Variation

In this section, we present more formal and more general conditions for population persistence in temporally varying environments, extending the results on population persistence and existence of positive steady states from Chaps. 3 and 4. We focus on random environments but mention the corresponding results for periodic variation as well. We begin with the work by Hardin et al. (1988a), which can be considered a spatially explicit extension of the work by Ellner (1984).

Hardin et al. (1988a) formulate their model as

$$N_{t+1}(x) = Q_t[N_t](x) = \int_\Omega K(x, y) R(\alpha_t, y) F(N_t(y)) \mathrm{d}y \,. \tag{16.20}$$

Environmental variation affects the dynamics via the "fertility" function $R(\alpha_t, y)$, where α_t, $t = 0, 1, 2, \ldots$ is a sequence of random variables. Density-dependent population limitation, modeled by F, is independent of time, as is dispersal,

modeled by K. The habitat is a (fixed) compact subset $\Omega \subset \mathbb{R}$ with nonempty interior. The initial condition and subsequent population densities are random functions in $\mathscr{C}_+(\Omega)$, the positive cone of continuous functions on Ω.

Hardin et al. (1988a) make the following assumptions:

(V1) Random variables α_t are iid from some index set $\mathscr{A}$.
(V2) Dispersal kernel K is a continuous and strictly positive function on $\Omega \times \Omega$.
(V3) For each $\alpha \in \mathscr{A}$, function $R(\alpha, x)$ is in $\mathscr{C}_+(\Omega)$, and there exist positive constants such that $0 < \underline{R} \leq R(\alpha, x) \leq \overline{R}$ for all $x \in \Omega$.
(V4) Function F is continuous, nonnegative, and bounded. It is differentiable at zero, and $F(0) = 0$. Furthermore, F is nondecreasing, and $F(x)/x$ is strictly decreasing for $x > 0$.

The first assumption implies that temporal variations are uncorrelated. The second condition indicates that within one dispersal period, an individual can move from any location in the habitat to any other location. The third assumption excludes the possibility that the population dies out in a single year. The conditions on the density-dependent growth limitations imply that the per capita yield decreases with density. They are satisfied by a Beverton–Hold type function; see (2.11).

Theorem 16.1 (Theorem 4.2 in Hardin et al. 1988a) *Suppose that conditions (V1)–(V4) are satisfied for (16.20) and that $N_0 \neq 0$ with probability one. Then N_t converges in distribution to a stationary distribution μ_*, which is independent of N_0. Furthermore, we have either $\mu_*(\{0\}) = 0$ or $\mu_*(\{0\}) = 1$.*

Just as in the deterministic case and in the nonspatial stochastic case, the difference between extinction and persistence is given by the behavior of the process at small densities. We denote by $Q_t'[0]$ the Fréchet derivative of Q_t at zero.

Theorem 16.2 (Lemma 5.1 and Theorem 5.3 in Hardin et al. 1988a) *Suppose that conditions (V1)–(V4) are satisfied. Then the limit*

$$\lambda = \lim_{t\to\infty} \| Q_t'[0] \circ Q_{t-1}'[0] \circ \cdots \circ Q_0'[0] \|^{1/t} \tag{16.21}$$

exists with probability one. Furthermore, if $\lambda < 1$, then $\mu_*(\{0\}) = 1$ and $N_t \to 0$ with probability one. Alternatively, if $\lambda > 1$, then $\mu_*(\{0\}) = 0$.

Both of these results hold under somewhat weaker conditions and for more general processes than the ones in (16.20) (Hardin et al. 1988a).

Hardin et al. (1988b) prove the corresponding results in T-periodic environments. They study the operator

$$Q_t[N] = \int_\Omega K(x, y) F_t(n(y))\, \mathrm{d}y\,, \tag{16.22}$$

where K denotes a dispersal kernel; F_t models reproduction in year t with $F_{t+T} = F_t$; and Ω is a bounded domain, as above. They consider the existence of a positive fixed point for the period-T-map $\overline{Q}^T = Q_{T-1} \circ \cdots \circ Q_0$, as well as its local and

global stability. Many of their results are contained in our Chap. 4, in particular Sect. 4.3 for global existence.

The persistence condition $\lambda > 1$ for the stochastic process is elegant theoretically but difficult to apply, even numerically. Jacobsen et al. (2015) present an equivalent condition that is computationally simpler to evaluate. Their model generalizes (16.20) in that it allows the dispersal kernel to vary in time. Their particular motivation was to study the effect of variable flow rates on the persistence of stream populations; see Sect. 12.2.

Consider the stochastic process

$$N_{t+1}(x) = Q_t[N_t](x) = \int_\Omega K_{\alpha_t}(x-y)F_{\alpha_t}(N_t(y))\mathrm{d}y, \qquad t = 0, 1, \ldots, \tag{16.23}$$

where α_t are iid random variables from some index set $\mathscr{A}$. We require the following generalizations of and additions to conditions (V1)–(V4):

(V2′) For each $\alpha \in \mathscr{A}$, K_α is a continuous function, and there exist constants such that $0 < \underline{K} \le K_\alpha \le \overline{K}$ for all α.

(V4′) For each $\alpha \in \mathscr{A}$, F_α is a nonnegative, continuous, and increasing function such that $F_\alpha(x)/x$ is decreasing and the right-sided limit $F'_\alpha(0)$ exists. Functions F_α are uniformly bounded by $m > 0$.

(V5) We have uniform limits $F_\alpha(x)/x \to F'_\alpha(0)$ as $x \to 0$ and uniform bounds $0 < \underline{F} \le F'_\alpha(0) \le \overline{F}$.

(V6) For $b = m\overline{K}|\Omega|$, there exists $\inf_{\alpha\in\mathscr{A}} F_\alpha(b) > 0$.

(V7) There exists $\alpha^* \in \mathscr{A}$ such that $Q_\alpha[N] \le Q_{\alpha^*}[N]$ for all $\alpha \in \mathscr{A}$ and nonnegative, continuous functions N on Ω.

Theorem 16.3 (Theorems 1 and 2 in Jacobsen et al. 2015) *Assume that conditions (V2′), (V4′), and (V5)–(V7) are satisfied. Then Theorems 16.1 and 16.2 hold for (16.23). Furthermore, the limit*

$$\Lambda = \lim_{t\to\infty} \Lambda(t) = \lim_{t\to\infty} \left[\int_\Omega n_t(x)\mathrm{d}x\right]^{1/t} \tag{16.24}$$

exists and is independent of n_0, where n_t is defined by $n_{t+1} = Q'_t[0]n_t$. Finally, $\Lambda = \lambda$.

The theory presented thus far considered temporal variation in growth and dispersal but assumed that the size and location of the habitat patch are fixed over time. There are many examples of natural habitats whose size and location vary within and between years. Wetlands are a particular example where surface area and depth vary according to rainfall and other climatic conditions. These observations motivate the study by Zhou and Fagan (2017), in which habitat size and location can vary with time. The authors implement a temporally varying habitat via a habitat quality function.

Zhou and Fagan (2017) analyze the model

$$N_{t+1}(x) = \int_{-\infty}^{\infty} K(x, y) H_t(y) F(N_t(y)) \mathrm{d}y \,, \tag{16.25}$$

where H_t is the temporally varying habitat quality function (compare Sect. 15.1) that determines the fraction of offspring produced at location y that survive to disperse. Function H_t has to be nonnegative and bounded above by unity. When H_t is the characteristic function of some fixed domain Ω, i.e., $H_t(x) = \chi_\Omega$, the model is equivalent to the basic IDE (3.1). When a domain of fixed length moves at constant speed, i.e., $H_t(x) = \chi_{[ct, L_0+ct]}$, we have the model from Sect. 12.3. When the domain length, L_t, varies with time, we may write $H_t(x) = \chi_{[0,L_t]}$. Zhou and Fagan (2017) consider this setting for a population whose habitat is the surface of a wetland. When not only the extent but also the quality vary in space and time, Zhou and Fagan (2017) suggest $H_t(x) = \exp(-x^2/\sigma_t^2)$ for a single wetland, where σ_t^2 is a random variable that indicates the extent in year t. The authors also consider more complex situations with, for example, two adjacent wetlands, modeled by a linear combination of two Gaussian functions, where the extent of each as well as the distance between them can vary over time.

The difficulty in analyzing model (16.25) lies in the variability of the domain with potentially infinite extent. If the support of all functions H_t is uniformly bounded, we can reduce model (16.25) to one on a compact set and obtain the same results as in Hardin et al. (1988a,b). Zhou and Fagan (2017) give conditions on the dispersal kernel and the habitat quality function under which the corresponding results hold even on the entire real line in a T-periodic environment. In particular, they show that, under some conditions, the stability of the zero solution is given by the spectral radius of the period-T-operator, and that the instability of zero implies that the (supremum norm of the) population will eventually be bounded below uniformly by some constant. Zhou and Fagan (2017) manage to calculate persistence conditions explicitly in two special cases. They define the "lower minimal habitat size" as an extension of the critical patch-size (Chap. 3) to periodic environments.

16.4 An Example with the Laplace Kernel

We illustrate some of the theory from the preceding section with a simple example. We assume that in year t, the habitat is an interval of length L_t. Inside the habitat, the growth function is the scaled Beverton–Holt function (2.13) with parameter $R_t > 1$; outside, the growth function is zero. Dispersal follows a Laplace kernel (2.27) with parameter a_t that can be interpreted as the root of the ratio α_t/D_t of the settling rate and the diffusion coefficient in a random walk; see Sect. 7.2. By scaling space in year t with L_t, we can write the equation on the fixed domain $[-1/2, 1/2]$ with kernel parameter $\tilde{a}_t = a_t L_t$ as

$$N_{t+1}(x) = \int_{-1/2}^{1/2} \frac{\tilde{a}_t}{2} e^{-\tilde{a}_t|x-y|} \frac{R_t N_t(y)}{1 + (R_t - 1)N_t(y)} \mathrm{d}y \,. \tag{16.26}$$

In the following, we will drop the tilde to ease notation. We are interested in population persistence. By the theoretical results in the preceding section, we need to study the stability of the zero state. Hence, we linearize the equation at low density. The resulting eigenvalue problem for the integral equation can be turned into an equivalent boundary-value problem for a differential equation (Jacobsen and McAdam 2014; Jacobsen et al. 2015), similar to the procedure in Chap. 3.

The Periodic Case

We consider a two-periodic environment, so that we have four model parameters: $a_{1,2} > 0$ and $R_{1,2} > 1$. The eigenvalue problem for the integral equation is given by

$$\lambda_p \phi(x) = R_1 R_2 \int_{-1/2}^{1/2} \int_{-1/2}^{1/2} \frac{a_1}{2} e^{-a_1|x-y|} \frac{a_2}{2} e^{-a_2|y-z|} \phi(z) \mathrm{d}y \mathrm{d}z \,. \tag{16.27}$$

To turn this equation into a boundary-value problem, we follow Jacobsen et al. (2015). We introduce the function

$$\psi(x) = R_1 \int_{-1/2}^{1/2} \frac{a_1}{2} e^{-a_1|x-y|} \phi(y) \mathrm{d}y \,. \tag{16.28}$$

Then ϕ satisfies (16.27) exactly if ϕ and ψ satisfy (16.28) and

$$\phi(x) = \frac{R_2}{\lambda_p} \int_{-1/2}^{1/2} \frac{a_2}{2} e^{-a_2|x-y|} \psi(y) \mathrm{d}y \,. \tag{16.29}$$

Differentiating twice, we find the second-order equations

$$\phi'' = a_2^2 \left(\phi - \frac{R_2}{\lambda_p} \psi \right) \quad \text{and} \quad \psi'' = a_1^2 (\psi - R_1 \phi) \tag{16.30}$$

for $x \in (-1/2, 1/2)$; compare (3.10). Differentiating again, these two equations can be turned into a single fourth-order equation for ϕ, namely

$$\phi^{(4)} - (a_1^2 + a_2^2)\phi'' + a_1^2 a_2^2 \left(1 - \frac{R_1 R_2}{\lambda_p} \right) \phi = 0. \tag{16.31}$$

We need to find boundary conditions. Two conditions are obtained exactly as in (3.11) by differentiating (16.28) and (16.29) once. We find

$$\phi'(-1/2) = -a_2\phi(-1/2)\,, \qquad \phi'(1/2) = a_2\phi(1/2)\,, \tag{16.32}$$

$$\psi'(-1/2) = -a_1\psi(-1/2)\,, \qquad \psi'(1/2) = a_1\psi(1/2)\,. \tag{16.33}$$

However, we need to find conditions for ϕ, not ψ. Differentiating (16.30) and substituting the above boundary conditions results in

$$\phi'''(-1/2) = a_1\phi''(-1/2) + a_2^2(a_2 - a_1)\phi(-1/2)\,, \tag{16.34}$$

$$\phi'''(1/2) = -a_1\phi''(1/2) - a_2^2(a_2 - a_1)\phi(1/2)\,. \tag{16.35}$$

The equation for ϕ has the bi-quadratic characteristic equation $r^4 - ar^2 + d = 0$, where

$$a = a_1^2 + a_2^2 \quad \text{and} \quad d = a_1^2 a_2^2 \left(1 - \frac{R_1 R_2}{\lambda_p}\right). \tag{16.36}$$

Just as in Chap. 3, we have $\lambda_p < R_1 R_2$, so that $a > 0$ and $d < 0$. We obtain two real and two purely imaginary roots:

$$r_1 = \sqrt{\frac{a + \sqrt{a^2 - 4d}}{2}}\,, \quad \mathrm{i}r_2 = \sqrt{\frac{a - \sqrt{a^2 - 4d}}{2}}\,, \tag{16.37}$$

and $r_3 = -r_1$, $r_4 = -r_2$. By symmetry, the eigenfunction can be written as

$$\phi(x) = c_1 \cosh(r_1 x) + c_2 \cos(r_2 x)\,. \tag{16.38}$$

To satisfy the boundary conditions, coefficients $c_{1,2}$ have to satisfy the equations

$$\begin{aligned} &[a_2 \cosh(r_1/2) + r_1 \sinh(r_1/2)]c_1 + [a_2 \cos(r_2/2) - r_2 \sin(r_2/2)]c_2 = 0\,, \\ &\Big[(a_1 r_1^2 + a_2^2(a_2 - a_1)) \cosh(r_1/2) + r_1^3 \sinh(r_1/2)\Big] c_1 \\ &\qquad + \Big[r_2^3 \sin(r_2/2) - (a_1 r_2^2 - a_2^2(a_2 - a_1)) \cos(r_2/2)\Big] c_2 = 0\,. \end{aligned} \tag{16.39}$$

For a nonzero solution, the determinant of the coefficient matrix has to vanish. This condition can be evaluated numerically.

We choose the same setup of a two-periodic environment as in the previous section. We write $a_{1,2} = \bar{a} \pm \epsilon_a$ and $R_{1,2} = \bar{R} + \epsilon_R$. Figure 16.3 shows that the dominant eigenvalue λ_p from (16.27) decreases as the variation ϵ_a in the kernel parameter and ϵ_R in the growth rate increases. Instead of the eigenvalue itself, we actually plot the square root of λ_p so that we can compare it with the average per generation rate of increase in the stochastic model below.

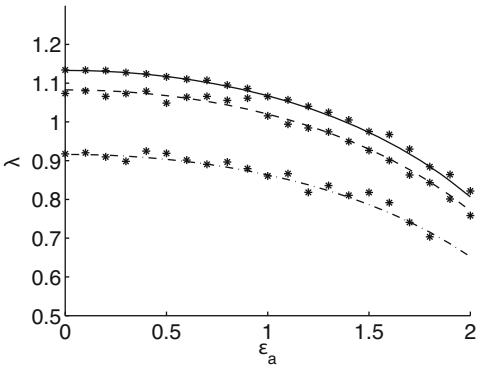

Fig. 16.3 Persistence condition for model (16.26) in the two-periodic and random cases. Solid curves show the square root of the eigenvalue, $\sqrt{\lambda_p}$, in (16.27). Stars stand for the numerically obtained value $\Lambda_T \approx \Lambda$ from (16.24). Parameters are $a_{1,2} = 2.7 \pm \epsilon_a$, and $R_{1,2} = \bar{R} \pm \epsilon_R$ with $\epsilon_R = 0$ (solid), $\epsilon_R = 0.5$ (dashed), and $\epsilon_R = 1$ (dash-dot).

The Stochastic Case

For random variation, we choose binary random variables a_t with values a_1, a_2 and R_t with values R_1, R_2 with equal probability. Then we numerically solve the linear equation

$$n_{t+1}(x) = R_t \int_0^1 \frac{a_t}{2} \exp(-a_t|x-y|) n_t(y) \mathrm{d}y \tag{16.40}$$

and approximate Λ from (16.24) by Λ_T for some large value of T. The results for different values of ϵ_a and ϵ_R are plotted as stars in Fig. 16.3. We note that the expected per generation rates of increase (or decrease) in the stochastic and periodic case are very close together. In fact, Jacobsen et al. (2015) find an even better agreement between their numerically calculated value Λ and the analytical expression $\sqrt{\lambda_p}$ in a slightly different setting. We note that persistence is harder to achieve and, in fact, fails, as the variation in each of the two parameters increases.

On a technical note, we found that the FFT algorithm from Sect. 8.2 could not (easily) provide the same accuracy as even the simple direct integration method from Sect. 8.3. Since the equation is linear, solutions grow or decay exponentially. Therefore, as the number of generations in the simulation grows, the values become either very large (if the solution is growing) or very small (if it is decaying), so that accuracy is difficult to maintain for large times. However, since we are interested in the limit of large times, there is some trade-off between accuracy of the computational steps and the number of time steps that one takes. To smooth out the results somewhat, we chose $T = 2000$ and averaged the value of the last 20 time steps.

16.5 Spread Under Temporal Variation

To study the effects of temporal variation on the spread rate of a population, we begin with the work by Neubert et al. (2000) (they provide corrected figures in an erratum) and study the IDE on the real line,

$$N_{t+1}(x) = Q_t[N_t](x) = \int_{-\infty}^{\infty} K_t(x-y)F_t(N_t(y))\mathrm{d}y\,. \tag{16.41}$$

Before we discuss results for the stochastic case, we briefly present some explicit results for the periodic case.

We assume that K_t and F_t are T-periodic functions of time. Furthermore, we assume that for each t, the growth function satisfies conditions (F1)–(F4) in Sect. 5.4. We also assume that for each t, the dispersal kernel is continuous, symmetric, and exponentially bounded. Then the period-T operator $\overline{Q}_t = Q_{T-1} \circ \cdots \circ Q_0$ satisfies the conditions of Theorem 5.1. Therefore, there exists a spreading speed, and this speed can be characterized as the slowest traveling-wave speed. Furthermore, the speed is linearly determined.

If we denote this speed by c^*T, where c^* is the average speed per generation, formula (5.17) gives the representation

$$c^* = \inf_{s>0} \frac{1}{s} \ln\left(\prod_{t=0}^{T-1} R_t M_t(s)\right)^{1/T} = \inf_{s>0} \frac{1}{s} \frac{1}{T} \sum_{t=0}^{T-1} \ln(R_t M_t(s))\,, \tag{16.42}$$

where M_t is the moment-generating function of kernel K_t and $R_t = F_t'(0)$. We denote by c_t^* the speed in a constant environment with conditions as in generation t. Since the infimum of the averages is generically greater than the average of the infima (unless the infima all occur at the same location), we have

$$c^* > \frac{1}{T} \sum_{t=0}^{T-1} \inf_{s>0} \frac{1}{s} \ln(R_t M_t(s)) = \frac{1}{T} \sum_{t=0}^{T-1} c_t^*\,. \tag{16.43}$$

Hence, the average speed per generation in the periodically varying environment is larger than the average of the speeds, c_t^*, that would occur in each of the corresponding constant environments. This statement can be strengthened as follows. Neubert et al. (2000) define the "instantaneous speed between generations" as

$$\bar{c}_t = \frac{1}{s^*} \ln(R_t M_t(s^*))\,, \tag{16.44}$$

where s^* is the argument that minimizes the expression in (16.42). Then, $\bar{c}_t > c_t^*$, which implies that the instantaneous speed between generations is greater than the

asymptotic speed would be in an environment of constant conditions of the most recent generation.

In the particular case that K_t are Gaussian kernels with variance σ_t^2, the procedure in Sect. 5.2 gives the exact expression for the average speed per generation as

$$c^* = \sqrt{2\langle\sigma_t^2\rangle_{\mathrm{a}} \ln(\langle R_t\rangle_{\mathrm{g}})}, \tag{16.45}$$

where $\langle\cdot\rangle_{\mathrm{a}}$ denotes the arithmetic mean and $\langle\cdot\rangle_{\mathrm{g}}$ the geometric mean.

Stochastic Environments

To consider spread rates for Eq. (16.41) in a stochastically varying environment, we study again the linearized IDE with growth rate $R_t = F_t'(0)$. Neubert et al. (2000) discuss the conditions for which the result is the spread rate in a corresponding nonlinear equation. We can approach the question of spread via the expectation or via direct calculation.

Taking expectations of Eq. (16.41) and assuming that growth and dispersal are uncorrelated with population density, we find

$$E[N_{t+1}](x) = \int_{-\infty}^{\infty} E[R_t K_t(x-y)]E[N_t(y)]\mathrm{d}y\,. \tag{16.46}$$

This is a deterministic equation for the "expectation wave." According to the theory in Chap. 5, there is a spreading speed, c^*. Formula (5.17) applies and results in the expression

$$c^* = \inf_{s>0} \frac{1}{s} \ln(E[R_0 M_0(s)])\,, \tag{16.47}$$

where M_0 is the moment-generating function of K_0. When growth and dispersal are uncorrelated, we obtain

$$c^* = \inf_{s>0} \frac{1}{s} \ln(E[R_0]E[M_0(s)])\,. \tag{16.48}$$

Positive correlations increase the spreading speed of the expectation wave.

For direct calculations, we choose the initial profile $N_0(x) = \exp(-sx)$ and calculate

$$N_1(x) = \int_{-\infty}^{\infty} R_0 K_0(x-y)\mathrm{e}^{-sy}\mathrm{d}y = \int_{-\infty}^{\infty} R_0 K_0(z)\mathrm{e}^{sz}\mathrm{d}y\ \mathrm{e}^{-sx} = R_0 M_0(s)\mathrm{e}^{-sx}. \tag{16.49}$$

Iteratively, we find

$$N_t(x) = \prod_{j=0}^{t-1} R_j M_j(s) \mathrm{e}^{-sx} . \tag{16.50}$$

Just as in Chap. 5, we define the extent of the population as $X_t = \sup_x \{N_t(x) \geq \tilde{N}\}$ for some threshold density, $\tilde{N}$. Unlike in Chap. 5, this quantity is now a random variable. Its explicit expression is

$$X_t = \frac{1}{s} \sum_{j=0}^{t-1} \ln(R_j M_j(s)) - \ln(\tilde{N})/s . \tag{16.51}$$

The mean speed per generation is the random variable

$$C_t = \frac{1}{t}(X_t - X_0) = \frac{1}{t} \sum_{j=0}^{t-1} \frac{1}{s} \ln(R_j M_j(s)) . \tag{16.52}$$

By the central limit theorem, C_t is asymptotically normally distributed with mean and variance given by

$$\mu(s) = \frac{1}{s} E(\ln(R_0 M_0(s))) \quad \text{and} \quad \sigma^2(s) = \frac{1}{ts^2} \mathrm{Var}(\ln(R_j M_j(s))) . \tag{16.53}$$

As before, the relevant speed is the minimum that occurs with respect to s; we denote the corresponding value by s^*. Hence, the speed that we are interested in is C_t with mean $\mu(s^*)$ and variance $\sigma^2(s^*)$. As $t \to \infty$, we find $\sigma^2(s^*) \to 0$, so that

$$C_t \to \bar{C} = \mu(s^*) = \inf_{s>0} \frac{1}{s} E[\ln(R_0 M_0(s))] . \tag{16.54}$$

Comparing this expression for $\bar{C}$ with c^* from (16.48), we apply Jensen's inequality again and find $\bar{C} \leq c^*$. In other words, the expectation wave is faster than almost every realization of the process. While the speed converges, i.e., $C_t \to \bar{C}$, the spatial extent, X_t, does not converge to $X_0 + \bar{C}t$. The reason for this lack of convergence is that the variance of the expression $C_t t + X_0$ grows linearly in t.

In Fig. 16.4, we plot the front location of two realizations of the process in an environment that switches between two states with probability 1/2. For comparison, we plot the front location in a two-periodic environment, as well as the average speed per generation from (16.45). We observe that one of the stochastic realizations is ahead of the periodic case and the other is behind, but all have the same slope. Hence, while the speed is predictable, the location is not. The plot on the right shows the front location (X_t) and the average speed (C_t) for 15 realizations of the process. Whereas the average speeds converge, the range of front locations spreads over time. Neubert and Parker (2004) review these results on spreading speeds in the context of risk analysis and apply the theory to the invasion of scotch broom.

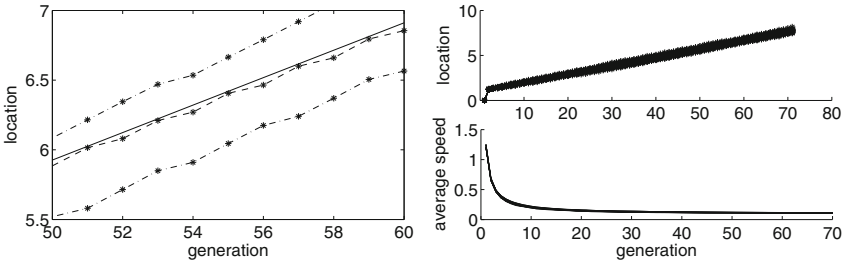

Fig. 16.4 **Left:** The location of the front as a function of time in a two-periodic environment (dashed) and two realizations in a random environment (dash-dot). The growth functions are Beverton–Holt functions $F(N) = R_j N/(1+N)$, and the kernels are Gaussian kernels with variance $\sigma^2_{1,2}$. The solid line represents the exact average speed per generation from (16.45). **Right:** The front location, X_t (top), and the average speed, C_t (bottom), for 15 realizations. Parameters are $R_{1,2} = 1.7 \pm 0.5$ and $\sigma^2_{1,2} = 0.01 \pm 20\%$.

16.6 Further Reading

Lewis and Pacala (2000) and Lewis (2000) formulate a discrete stochastic process for the reproduction and dispersal of individuals and analyze its spreading behavior. They derive a set of moment equations, which turn out to be IDEs. In fact, the equation for the first moment of the linear process is precisely the equation for the expectation wave (16.46). They study permanence of form for the spreading population and use moment closure techniques and comparison methods to bound spread rates. Snyder (2003) continues this theory and shows that stochasticity can slow invasions but concludes that the effect is relatively weak. Kot et al. (2004) link individual-based simulations and IDEs via branching random walks to study the effect of demographic stochasticity on the speed of invasions. They find that stochasticity does not slow the overall asymptotic speed and that accelerating invasions can occur with stochasticity as well.

Several authors consider the spread of structured populations in periodic and stochastic environments. Caswell et al. (2011) extend their previous sensitivity analysis for spread rate in structured population models (see Neubert and Caswell 2000a) to periodic and stochastic environments. Simultaneously but independently, Schreiber and Ryan (2011) derive formulas for invasion speeds for stage-structured IDEs in stochastic environments. They show that invasion speeds are asymptotically normally distributed and that, as is the case for unstructured populations, the variance decreases over time (Fig. 16.4). Increased variation in fecundity decreases invasion speeds, but correlations between fecundity and dispersal determine by how much. Related work for spatial integral projection models can be found in Ellner and Schreiber (2012).

Ding et al. (2013) prove the existence of spreading speeds in time-periodic IDEs in spatially constant or spatially periodic environments. They show that temporal heterogeneity will slow down invasions if space is homogeneous but

can speed up invasions if space is also heterogeneous. Jacobsen et al. (2015) determine persistence criteria on a bounded interval with temporally varying unidirectional flow. Bouhours and Lewis (2016) consider a moving-habitat model with stochasticity and determine persistence conditions. Zhou and Fagan (2017) consider temporally varying habitat size and quality and extend the theory by Hardin et al. (1988a) to the case where the habitat may be unbounded. They give several examples of wetland habitats that vary with seasonal rainfall, and they calculate long-term persistence conditions. Reimer et al. (2017) compare and contrast several approaches to determining persistence conditions of populations on a bounded domain under stochasticity. They use individual-based model simulations, Galton–Watson branching processes, and a deterministic IDE. They find that the critical patch-size for the stochastic models is typically larger than that for the deterministic model.

Several authors apply stochastic IDEs to various ecological questions and base their investigation largely on numerical simulations. Mahdjoub and Menu (2008) consider the question of whether and how diapause can affect the population spread of the chestnut weevil (*Curculio elephas*). They consider equations for developing individuals and individuals in diapause. Only the former disperse. They find that prolonged diapause will reduce spread in a constant environment but can increase spread in a temporally varying environment. Gilioli et al. (2013) model the spread of the chestnut gall wasp (*Dryocosmus kuriphilus*) in Europe. They use a deterministic IDE for short-distance dispersal, coupled with a stochastic component for long-distance dispersal, to capture the observed stratified dispersal pattern. Gharouni et al. (2017) formulate a three-stage model for green crab and study the effect of stochastic variation on the spread of the crab against the dominant current. Stochasticity may help the population spread "upstream"; see Sect. 12.2.

Jacobs and Sluckin (2015) study the effect of demographic stochasticity on accelerating invasions. They compare individual-based simulations on a lattice with predictions from a deterministic IDE model. When the dispersal kernel is heavy tailed, the IDE predicts accelerating invasions, but most of the corresponding lattice models appear to have constant-speed invasions.